Redox Biology 36 (2020) 101648

Contents lists available at ScienceDirect

Redox Biology

journal homepage: www.elsevier.com/locate/redox

CMS121, a fatty acid synthase inhibitor, protects against excess lipid peroxidation and inflammation and alleviates cognitive loss in a transgenic mouse model of Alzheimer's disease

Gamze Ates, Joshua Goldberg, Antonio Currais, Pamela Maher *

Cellular Neurobiology Laboratory, The Salk Institute for Biological Studies, La Jolla, CA, USA

ARTICLE INFO

Keywords:
Alzheimer's disease
Cognition
Lipid peroxidation
Fatty acid synthase
Ferroptosis
Oxytosis

ABSTRACT

The oxidative degradation of lipids has been shown to be implicated in the progression of several neurodegenerative diseases and modulating lipid peroxidation may be efficacious for treating Alzheimer's disease (AD). This hypothesis is strengthened by recent findings suggesting that oxytosis/ferroptosis, a cell death process characterized by increased lipid peroxidation, plays an important role in AD-related toxicities. CMS121 is a small molecule developed against these aspects of neurodegeneration. Here we show that CMS121 alleviates cognitive loss, modulates lipid metabolism and reduces inflammation and lipid peroxidation in the brains of transgenic AD mice. We identify fatty acid synthase (FASN) as a molecular target of CMS121 and demonstrate that modulating lipid metabolism through the inhibition of FASN protects against several AD-related toxicities. These results support the involvement of lipid peroxidation and perturbed lipid metabolism in AD pathophysiology and propose FASN as a target in AD-associated toxicities.

1. Introduction

The World Health Organization acknowledges that Alzheimer's disease (AD) is a priority for public health [1]. Yet, there are still no disease-modifying drugs to treat it. Hundreds of drug candidates have failed during clinical development and since 2003 no new drug candidates against AD have been approved by the FDA [2]. Currently approved therapies are only symptomatic, with limited improvements in memory. Efforts to understand the mechanisms underlying cell damage and death in AD have highlighted the detrimental effects of excessive lipid peroxidation [3,4]. Moreover, it is likely to be an early feature of the disease, as post-mortem brain samples from subjects with mild cognitive impairment already show increased levels of lipid peroxidation, which are maintained throughout disease progression [5,6].

CMS121 is a small molecule and derivative of the flavonoid fisetin, developed by a drug discovery paradigm based on phenotypic screening assays that mimic several aspects of AD-related toxicities such as (i) ischemia, (ii) inflammation and (iii) endogenous oxidative stress [7]. The latter is induced by inhibiting the activity of the glutamate/cystine antiporter system x_c^-, consequently depleting cells of glutathione (GSH), the major endogenous intracellular antioxidant, and triggering a non-apoptotic, regulated cell death process called oxytosis [8] or ferroptosis [9]. GSH depletion leads to increased levels of reactive oxygen species (ROS), followed by high levels of lipid peroxidation and eventually cell death [10]. CMS121 is able to rescue cells from oxytotic/ferroptotic cell death [7].

Here, we demonstrate the effects of CMS121 on cognitive dysfunction in APPswe/PS1ΔE9 transgenic mice. Treatment with CMS121 was started at 9 months, an age when pathology is significantly advanced [11]. Metabolomic and protein analyses were performed to unravel the mechanism through which CMS121 maintains cognitive function in mice. Finally, we identify the putative target of CMS121 and its involvement in AD-related toxicities and oxytosis/ferroptosis-induced lipid peroxidation.

2. Results

2.1. CMS121 alleviates cognitive dysfunction in APPswe/PS1ΔE9-transgenic mice

Since fisetin, the parent compound of CMS121, did not affect the number of plaques or the levels of soluble and insoluble amyloid beta in the same AD mouse model [12] and amyloid peptide accumulation has been the target of numerous clinical trials that have failed to provide

* Corresponding author.
E-mail address: pmaher@salk.edu (P. Maher).

https://doi.org/10.1016/j.redox.2020.101648
Received 27 May 2020; Received in revised form 15 July 2020; Accepted 17 July 2020
Available online 21 July 2020

benefits in AD patients, we focused here on changes in cognition. In order to investigate if CMS121 improves cognitive deficits in AD mice, we subjected APPswe/PS1ΔE9 transgenic mice to several behavioral tests modelling different aspects of cognition known to be affected in AD. Mice were tested after a 3-month treatment regimen of 400 ppm CMS121 (approximately 34 mg/kg/day). Treatment started at the age of 9 months. As previously reported by our lab, mice at that age already showed signs of cognitive deficits [12].

Spatial learning and memory were tested in the 2-day Morris Water Maze (MWM) [13]. During the training phase (day 1), when the platform was visible, all mice were able to locate the platform after the fourth trial. There were no differences in escape latency between the different groups (Fig. 1A). However, it took a significantly longer amount of time for the untreated AD mice to locate the platform during the trial phase (day 2) when the platform was hidden, suggesting a deficit in spatial learning. In contrast, AD mice treated with CMS121 performed as well as the WT mice.

In humans, AD patients present a lack of restraint, referred to as disinhibition [14]. A disinhibition phenotype was also detected in our untreated AD mice that spent significantly more time in the open arms of the elevated plus maze (EPM) than their WT counterparts. However, no differences between WT and CMS121-treated AD mice were detected (Fig. 1B).

AD mice also showed deficiencies in contextual memory, as tested by the fear conditioning assay. On day 2 of this assay, mice were placed in the same context as the previous day but did not receive the aversive stimulus. The time AD mice spent freezing was significantly shorter than the WT mice. CMS121-treated AD mice did not show this deficiency, when compared to WT mice (Fig. 1C). Thus, in all three behavioral assays, the CMS121-treated AD mice performed significantly better than the untreated AD mice. This suggests that CMS121 may be effective against a variety of AD-associated cognitive deficits.

2.2. *CMS121 prevents excess lipid peroxidation and reduces neuroinflammation*

Lipid peroxidation is considered an important hallmark of AD cellular pathology [6,15,16]. Not only can peroxidation of membrane lipids become harmful to lipid bilayer function and cellular integrity but the by-products of lipid peroxidation can act as electrophilic aldehydes to crosslink with DNA or covalently bind to amino acids, thus interfering with nucleic acid and protein structure and function. Additionally, they can act as signalling molecules able to induce inflammation [17–19]. We assessed the ability of CMS121 to prevent an increase in lipid peroxidation in cells and animals. In the HT22 neuronal cell line, increased lipid peroxidation was induced by RSL3, an inhibitor of glutathione peroxidase 4 (GPX4). GPX4 is an important detoxifier of lipid peroxides and a key enzyme in ferroptosis/oxytosis [10]. CMS121 was able to prevent the increase in lipid peroxidation by RSL3 (Fig. 2A). CMS121 also inhibited lipid peroxidation in BV2 microglial cells activated by LPS (Fig. 2B). An important cytotoxic by-product and marker of lipid peroxidation is 4-hydroxynonenal (4HNE) [20]. *In vivo*, an increase of 4HNE protein adducts in the hippocampus of untreated AD mice was observed and CMS121 treatment decreased hippocampal 4HNE protein adduct levels to those of untreated WT mice (Fig. 2C).

Lipid peroxides can be formed non-enzymatically and enzymatically. The most important group of enzymes catalysing the dioxygenation of lipids – mainly of polyunsaturated fatty acids (PUFAs)- to form lipid hydroperoxides, are lipoxygenases (LOX). LOX enzymes can act on both fatty acids in phospholipids and free fatty acids to generate eicosanoids [21]. Eicosanoids are bioactive lipid mediators derived from PUFAs such as arachidonic acid (AA) and serve as regulators of the inflammatory response, with both pro- and anti-inflammatory effects. LOX enzymatic activity has been directly linked to oxytosis/ferroptosis-induced lipid peroxidation and cell death [8,10,22–24]. The only LOX gene expressed in HT22 cells is *ALOX15B* which encodes 15LOX2, suggesting that 15LOX2 is enough to maintain the cell death pathway [10,24]. In AD, 15LOX2 has been implicated in inflammation and its levels are increased in human AD patients [25]. Similarly, our results demonstrate an increase of 15LOX2 in the hippocampus of untreated AD mice. CMS121 treatment reduced the levels of 15LOX2 to those of untreated WT mice (Fig. 2D).

Another marker of inflammatory stress in the brain is glial fibrillary acidic protein (GFAP) and lipid peroxidation is known to increase its levels in the hippocampus [26]. In our study we also detected an increase in GFAP in the hippocampi of AD mice and treatment with CMS121 decreased its levels (Fig. 2E). These results suggest that CMS121 has anti-inflammatory effects *in vivo* that may be linked to its

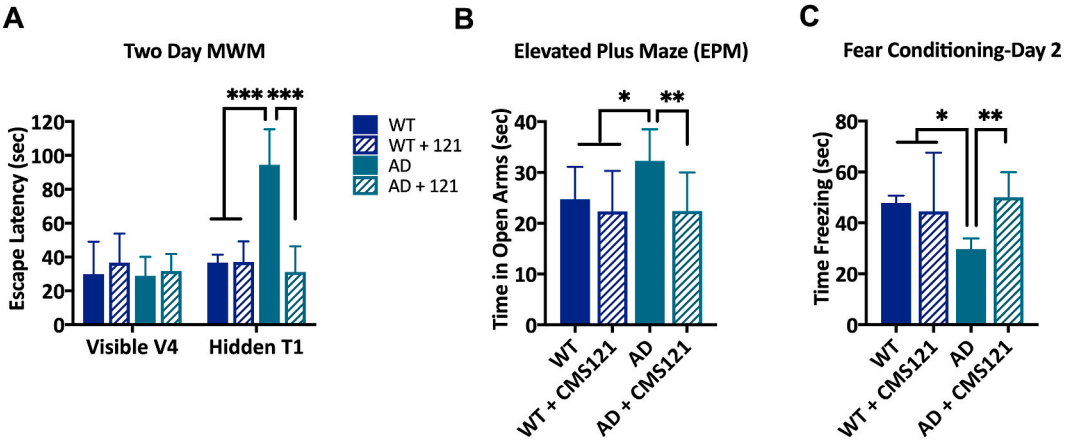

Fig. 1. CMS121 alleviates cognitive dysfunction in APPswe/PS1ΔE9 transgenic AD mice. After 3 months of treatment with CMS121, the spatial memory (**A**), the anxiety response (**B**) and the contextual memory (**C**) in 12 months old APPswe/PS1ΔE9 transgenic AD mice were normalized to age-matched WT levels. **A.** While all mice were able to locate the visible platform after 4 trials (V4) in the Morris Water Maze (MWM), untreated AD mice spent significantly more time locating the hidden platform. In contrast, CMS121-treated AD mice could, identical to WT mice, locate the platform after only one trial (T1). **B.** The disinhibition response was assessed by measuring the time the mice spent in the open arms of the elevated plus maze (EPM) over a 5min trial. Untreated AD mice spent a significantly longer amount of time in the open arms, compared to the other test groups, confirming the disinhibition phenotype seen in AD. **C.** Similarly, the contextual memory of AD mice was impaired, as measured by the fear conditioning test. The first day, the mice received an aversive stimulus after receiving a tone. After 24h, the mice were placed back in the same chamber for 120s but without the tone. The time the untreated AD mice spent frozen was significantly lower than the other test groups, suggesting a loss of contextual memory. CMS121 treatment normalized contextual memory back to baseline WT levels. (*p<0.05, **p<0.01, ***p<0.001, one-way ANOVA, Tukey's post-hoc test, n = 12).

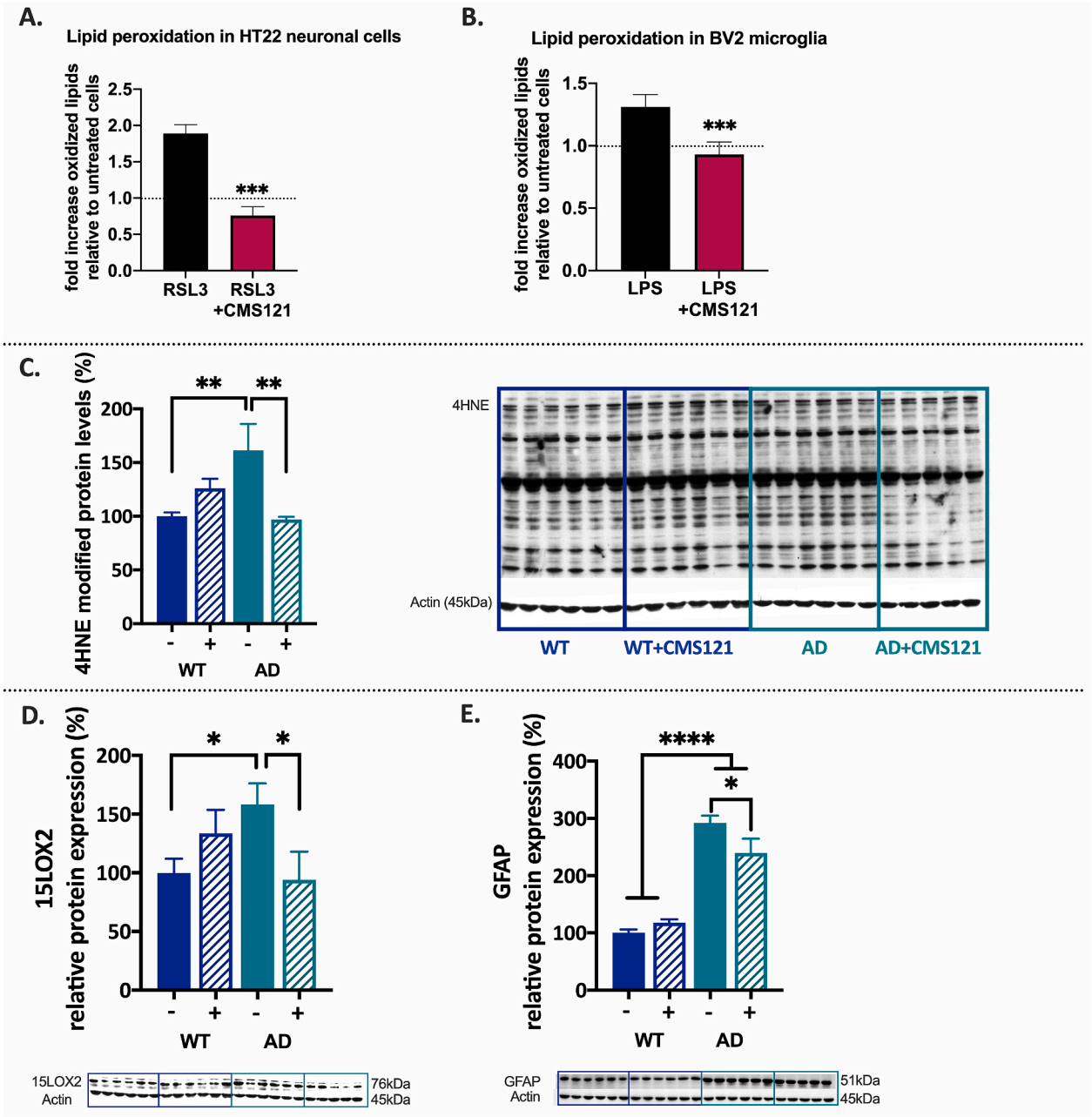

Fig. 2. CMS121 decreases lipid peroxidation and has anti-inflammatory properties. Using Bodipy 581/591 reagent we found that CMS121 prevents the increase in lipid peroxidation induced by the GPX4 inhibitor RSL3 in HT22 neuronal cells **(A)** and by LPS in BV2 microglial cells **(B)**. Results are expressed as mean fold changes ±SD; relative to untreated control cells: fold changes are thus calculated by using untreated control cells as baseline (***$p<0.001$, T-test, n = 3–4). **C.** Relative levels of 4-hydroxynonenal (4HNE) protein adducts as a measure of lipid peroxidation are increased in untreated AD compared to untreated WT mice. Treatment of AD mice with CMS121 reduced 4HNE adduct levels back to WT levels. To measure the level of 4HNE protein adducts, the optical density of the entire lane was determined (the whole lane was considered as a single band) and normalized against the respective actin levels. CMS121 decreases 15LOX2 (**D**) and GFAP (**E**), both markers of inflammation in the hippocampi of AD mice. Results are expressed as mean ± SEM (*$p<0.05$, **$p<0.01$, ***$p<0.001$, ****$p<0.0001$. One-way ANOVA, n = 5–6).

preventative action on increased lipid peroxidation in AD.

2.3. Intraneuronal amyloid beta-induced increase in eicosanoids is countered by CMS121

To examine this idea further we used the human MC65 cell line which is a tetracycline(Tet)-inducible model of intraneuronal Aβ toxicity. When Tet is withdrawn, the cells express the C-99 fragment of APP which is subsequently cleaved to Aβ by γ-secretase, leading to amyloid-induced inflammation followed by proteotoxicity and eventually cell death [27], providing us with a unique *in vitro* model to directly investigate the responses provoked by intracellular Aβ and the effects of CMS121 on them.

We found that CMS121 prevents Aβ accumulation (Fig. 3A) and inhibits cell death (Fig. 3B) in the MC65 cells. In this cell system, we also investigated eicosanoids, which can serve as markers of both enzymatic and non-enzymatic lipid peroxidation. In the supernatants of the MC65 cells, we detected 43 eicosanoids (Fig. 3C). The majority of those detected (29/43) are derived from AA (Fig. 3D), followed by eicosanoids derived from linoleic acid (LA, 11/43) and docosahexaenoic acid (DHA,

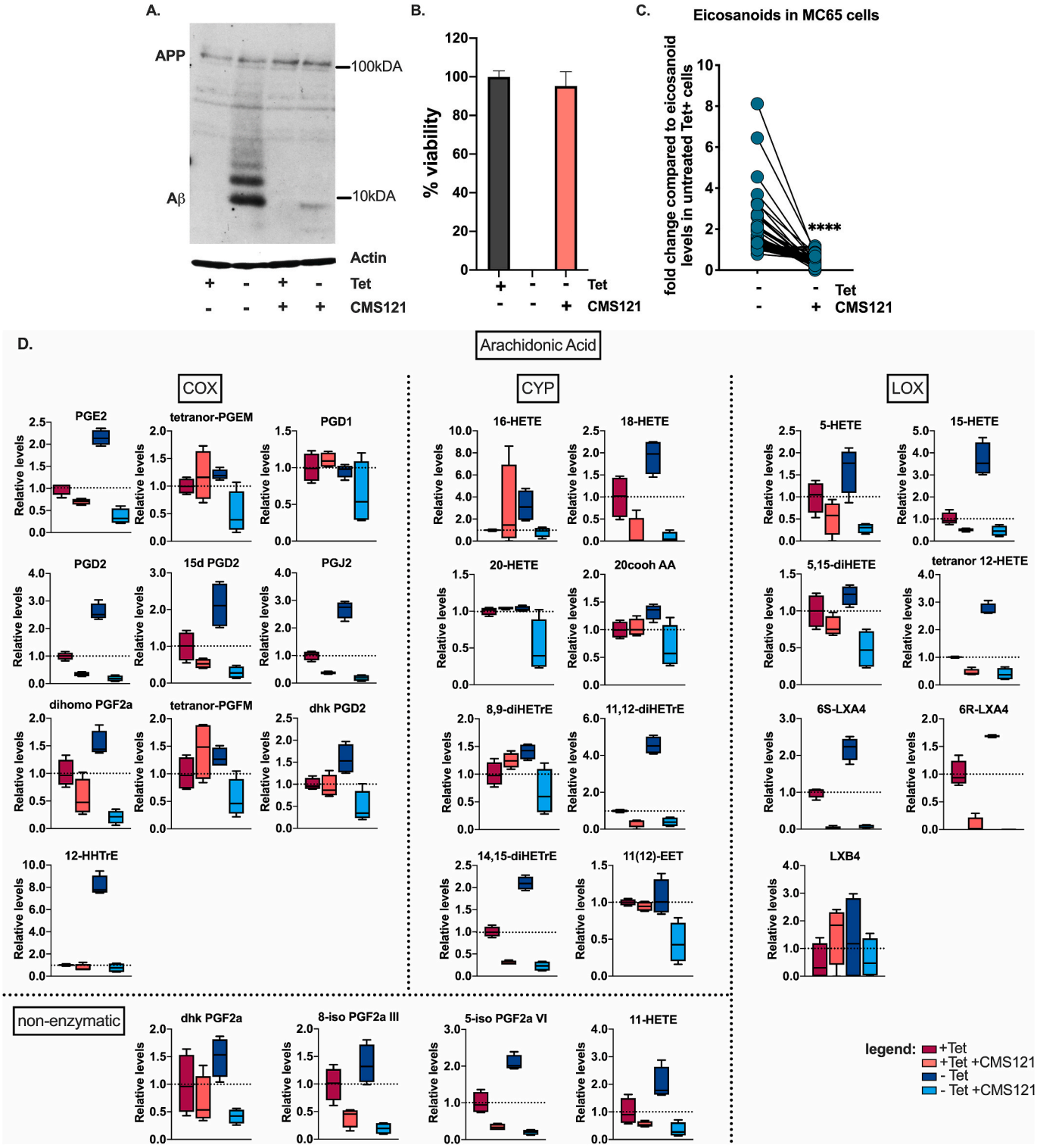

Fig. 3. Intraneuronal Aβ increases eicosanoids and this is countered by CMS121.
A. Representative blot of intracellular Aβ induction after Tet removal (Tet-) in MC65 cells. CMS121 prevents the accumulation of Aβ. **B.** CMS121 prevents cell death induced by intracellular Aβ in MC65 cells (n = 3). **C.** Eicosanoid analysis of MC65 cells shows a general increase in eicosanoid levels secreted into the culture medium by cells when Aβ toxicity is induced (Tet-). Treatment of cells with CMS121 prevents this increase (Tet- + CMS121). Results are expressed as fold changes normalized over Tet + baseline levels. Every dot represents the average fold change of a single eicosanoid (****$p<0.0001$, Wilcoxon matched-pairs signed rank test, n = 4). **D,E.** Individual eicosanoids derived from arachidonic acid **(D)**, linoleic acid **(E)** and docosahexaenoic acid **(E)** organized by the main enzymatic system involved in the metabolism of the respective eicosanoid (COX: cyclooxygenase; CYP: cytochrome p450; LOX: lipoxygenase). Relative lipid levels, normalized against + Tet controls, are depicted (n = 4).

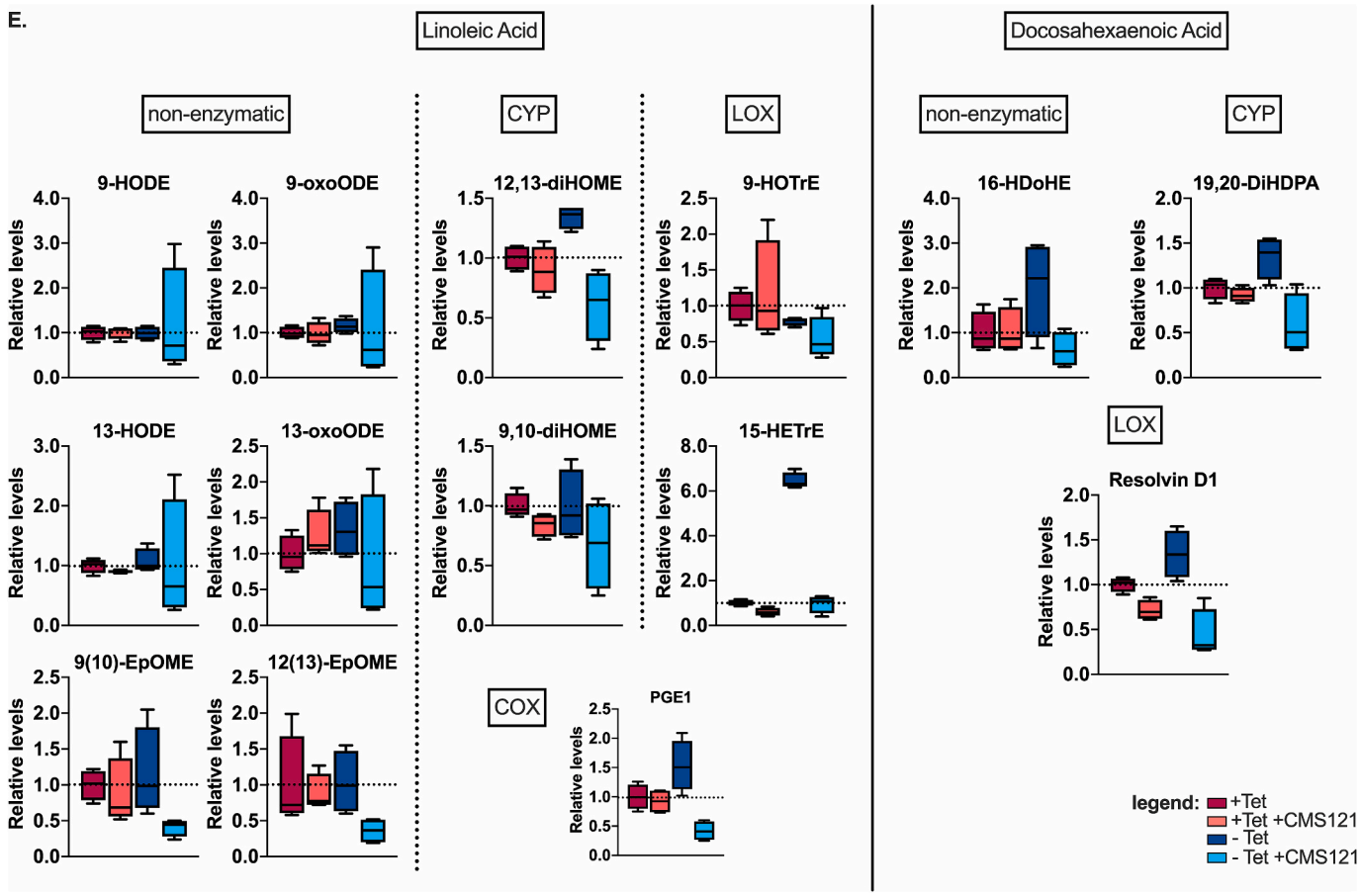

Fig. 3. (*continued*).

3/43) (Fig. 3E). An increase in all eicosanoids was observed after induction of intracellular Aβ. This increase was prevented by CMS121, irrespective of the origin or (enzymatic or non-enzymatic) pathway involved in their synthesis (Fig. 3C–E). These data demonstrate that intracellular Aβ leads to a general increase in eicosanoids and their precursors, and show that CMS121 has a broad cytoprotective and anti-inflammatory effect, suggesting a more general mechanism beyond that of a specific LOX inhibition.

2.4. CMS121 modulates lipid metabolism

To further investigate CMS121's mechanism of action, we performed an untargeted metabolomics analysis on the cortex of the same mice used for cognitive function assessment. Random forest analysis using the top differentially regulated metabolites revealed a consistent effect on lipid metabolites (Fig. 4A). Based on these results and the direct link between lipid metabolism and lipid peroxidation, we examined how levels of different lipid groups changed in treated and untreated AD mice. In untreated AD mice, increased levels of total lipid-related metabolites were observed as compared to the CMS121 treatment group (Fig. 4B).

To determine if CMS121 had specific effects on lipid metabolite subsets in AD, we analyzed each subgroup individually. Relative levels of endocannabinoids, fatty acids, and PUFAs were significantly higher in untreated AD mice as compared to CMS121-treated AD mice (Fig. 4C). Only ceramide levels showed significantly increased fold changes in CMS121-treated AD mice. No significant group changes were observed in lysophospholipids, sphingolipids and in metabolites related to fatty acid metabolism. Although no changes in select eicosanoids were observed in these mice, this can be attributed to the much more limited panel of eicosanoids examined relative to those tested in the MC65 cells.

The general increase in lipids correlated with an increase in both palmitate (Fig. 4D) and FASN protein (Fig. 4E) levels in the AD mice. FASN is a key enzyme in the synthesis of lipids, where it utilizes NADPH to catalyze the formation of palmitate from acetyl-CoA and malonyl-coA. Palmitate is then further elongated and desaturated to form mono- and polyunsaturated fatty acids. Although CMS121 seemed to increase FASN protein levels in WT mice, this effect was not statistically significant and CMS121 did not alter FASN protein levels in the AD mice (Fig. 4E). CMS121 did normalize palmitate levels in AD mice to those seen in control mice (Fig. 4D). These results further support a role for the dysregulation of lipid biosynthesis in AD mice and suggest that its prevention is implicated in CMS121's protective effects.

2.5. FASN is a target of CMS121

To identify the target through which CMS121 regulates lipid metabolism, we performed drug affinity responsive target stability (DARTS) analysis on HT22 and HeLa cells. Mass spectrometry identified FASN as a top hit. In fact, FASN is the only protein present in the top 3 targets for both cell lines (Table 1). The entire data set can be consulted via: https://data.mendeley.com/datasets/v6gjkzggfr/draft?a=587e71a7-f962-414f-869f-54f4ed7009d4 https://doi.org/10.17632/v6gjkzggfr.1). We then measured the enzymatic activity of FASN in HT22 cell lysates. Fig. 5A demonstrates a CMS121-mediated, dose-dependent decrease in FASN activity, confirming that FASN is indeed a biological target of CMS121.

To determine whether the observed protective effects of CMS121 are related to its inhibition of FASN, we knocked down *FASN* in HT22 cells and tested the sensitivity of these cells against three inducers of

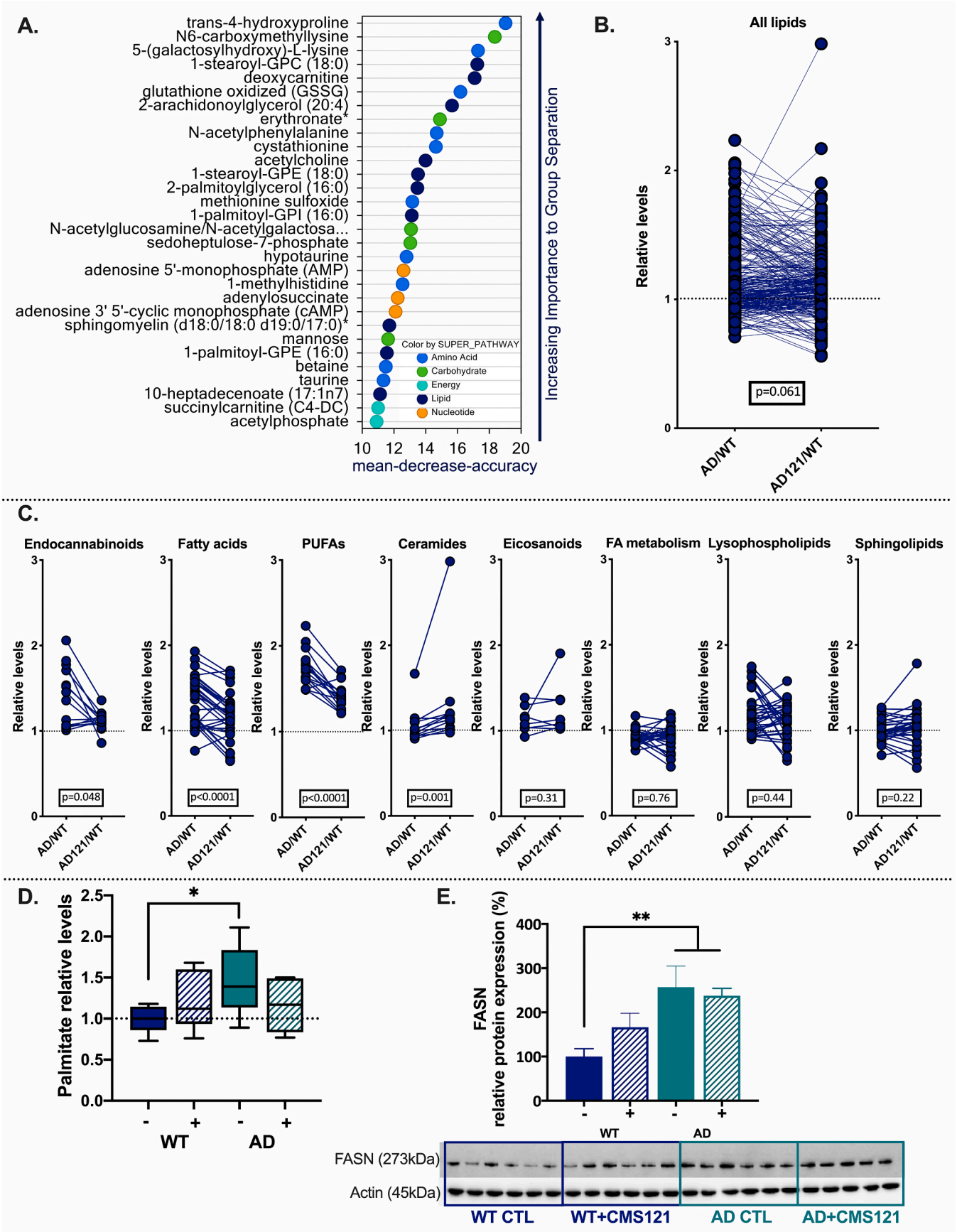

(caption on next page)

Fig. 4. Lipid metabolism is dysregulated in AD and CMS121 affects several lipid classes in mouse cortex. **A.** Random forest analysis of the top 30 metabolites indicates the importance of lipids in the separation of the different treatment groups. **B.** In general, metabolites classified as lipids are more elevated in untreated AD mice than CMS121-treated AD mice. **C.** Levels of endocannabinoids, fatty acids, PUFAs and ceramides are most clearly affected by CMS121. Eicosanoids, metabolites related to fatty acid (FA) metabolism, lysophospholipids and sphingolipids are not significantly altered in AD or affected by CMS121 treatment. Lipid levels are expressed as relative levels, normalized against untreated wildtype mice (WT). Statistical significance is determined by the Wilcoxon matched-pairs signed rank test. Cortices of 5 animals per treatment group were analyzed; each datapoint represents the average relative level of a specific metabolite. Only the most important lipid groups are presented. The entire metabolomics data set is available via https://data.mendeley.com/datasets/v6gjkzggfr/draft?a=587e71a7-f962-414f-869f-54f4ed7009d4 https://doi.org/10.17632/v6gjkzggfr.1. **D-E.** Palmitate levels (**D**) as well as protein levels of FASN (see also blot below graph) (**E**), support a general increase in lipid levels in AD brains. Results are expressed as mean ± SEM for relative protein levels, and as box and min. to max. whisker plots for palmitate (*p<0.05, **p<0.01, one-way ANOVA, n = 5–6).

Table 1
Top 3 proteins protected by CMS121 from pronase digestion in HT22 and HeLa cells.

HT22	spectral counts		fold change	
	control	**CMS121**	**CMS121/ control**	**description**
	14	110	7.9	Filamin-B OS = Mus musculus GN = Flnb PE = 1 SV = 3
	48	136	2.8	Filamin, alpha OS = Mus musculus GN = Flna PE = 1 SV = 1
	47	**128**	**2.7**	**Fatty acid synthase OS = Mus musculus GN = Fasn PE = 1 SV = 2**
HeLa	**spectral counts**		**fold change**	
	control	**CMS121**	**CMS121/ control**	**description**
	34	141	4.15	Plectin OS=Homo sapiens GN = PLEC
	41	**106**	**2.59**	**Fatty acid synthase OS=Homo sapiens GN = Fasn PE = 1 SV = 3**
	93	209	2.25	Myosin-9 OS=Homo sapiens GN = MYH9 PE = 1 SV = 4

Mass spectrometry on proteins protected from pronase digestion identified putative target proteins of CMS121. Proteins are considered of interest when they have spectral counts of >100 after CMS121 treatment and at least a 2-fold enrichment in the CMS121-treated samples, compared to vehicle controls, in both cell lines. This threshold was chosen in order to minimize the chances of detecting noise. FASN is the only protein present in the top 3 targets of both cell lines.

oxytosis/ferroptosis, glutamate, erastin and RSL3 (Fig. 5B–E). With all three inducers, knockdown of *FASN* significantly protected the HT22 cells from oxytosis/ferroptosis. However, in both glutamate- and erastin-induced oxytosis/ferroptosis, CMS121 enhanced protection after *FASN* knockdown (Fig. 5F and G). Interestingly, CMS121 did not offer additional protection against RSL3-induced oxidative cell death following *FASN* knockdown (Fig. 5H).

Next, we set out to determine if *FASN* knockdown could also prevent 4HNE adduct formation during RSL3 toxicity. RSL3 exposure to control cells caused an increase in levels of 4HNE-adducts, which were reduced by CMS121 treatment. *FASN* knockdown led to a significant decrease in baseline levels of 4HNE adducts. The same concentration of RSL3 did not significantly increase lipid peroxidation after *FASN* knockdown and CMS121 did not further decrease lipid peroxidation in these cells (Fig. 5I and J). Furthermore, a significant correlation was observed between *FASN* and 4HNE levels ($r = 0.86$, $p<0.0001$) (Fig. 5K).

Several reports have implicated FASN in the regulation of inflammatory stimuli in macrophages [28,29]. We investigated whether FASN exhibits similar properties in microglia, the resident macrophages of the brain. Levels of iNOS, TNFα and COX2, all known to play a role in neuroinflammation and AD pathology [30–32], were measured after knockdown of *FASN* and compared to CMS121-treated BV2 microglia. LPS treatment increased the inflammatory markers (Fig. 5L–U) and CMS121 (Fig. 5L–O) and *FASN* knockdown (Fig. 5P–U) both prevented this increase, supporting the idea that the anti-inflammatory effects of CMS121 are largely dependent on FASN inhibition.

Importantly, FASN protein levels were also significantly increased in AD patients (Fig. 5V). In addition, knocking down *FASN* in MC65 cells prevented cell death, implying a neuroprotective role of FASN inhibition in intracellular Aβ toxicity (Fig. 5W) and further linking CMS121 activity to the inhibition of FASN. Altogether, these results identify FASN as a target of CMS121 that mediates its effects on lipid peroxidation and inflammation.

3. Discussion

AD drug discovery has mainly focussed on targeting the amyloid pathway. Failed clinical trials, however, have led to a reassessment of the amyloid hypothesis, yet alternative targets to treat AD are scarce. Our lab has a unique *in vitro* screening platform that tests compounds for their ability to protect against multiple toxicities related to AD [7]. This strategy has led to the development of J147 as a drug candidate against AD, simultaneously delivering the mitochondrial ATP synthase as a new drug target [13,33]. J147 is currently in phase I clinical trials for AD (NCT03838185). CMS121 is the result of a similar optimization strategy to generate a compound with pharmacological properties directed towards the treatment of neurodegenerative diseases with an oxidative stress component [34]. CMS121 has already shown beneficial effects on cognitive function in a mouse model of accelerated aging, even when administered at advanced stages of aging [35].

Here we explore the potential of CMS121 in the treatment of AD in the APPswe/PS1ΔE9 double transgenic mouse model and identify the possible target and mechanisms through which it reduces AD related cognitive dysfunction. We tested the effects of CMS121 on spatial memory, contextual memory and disinhibition. In all three paradigms, AD mice that had received treatment performed as well as age-matched WT mice, while untreated AD mice showed a clear dysfunction in every test. These results are comparable to a previous study published on the effect of the parent compound fisetin on memory in the same mouse model [12], confirming that CMS121 maintains the beneficial effects of fisetin on memory and cognition in AD mice.

We also show that CMS121 is able to prevent the increase in lipid peroxidation in both neuronal and microglial cells. Lipid peroxidation involves the interaction of ROS with (poly) unsaturated fatty acids. An excess of lipid peroxides becomes toxic to cells as it can affect the membrane structure, and consequently many bioenergetic and signalling processes and even the integrity of the cellular membranes. Additionally, some of the by-products of lipid peroxidation are reactive compounds that can crosslink to DNA and proteins, affecting their normal function [15]. The brain is particularly vulnerable to lipid peroxidation as it is rich in PUFAs and has a high oxygen consumption [36]. Numerous studies show increased levels of lipid peroxidation in the brains of patients with cognitive impairment and AD [6,37–42]. As a result, several antioxidants and metal chelators-iron and copper are catalysts for the formation of free radicals-have been proposed as possible treatment strategies in AD, but with minimal success. Vitamin E and C supplementation, for instance, did not alter AD disease progression [43]. The iron chelator deferiprone is currently undergoing a phase 2 clinical trial for AD (NCT03234686). Since lipid peroxides are the result of a chain reaction initiated by ROS but further propagated independently of ROS, the formation of lipid peroxides can continue

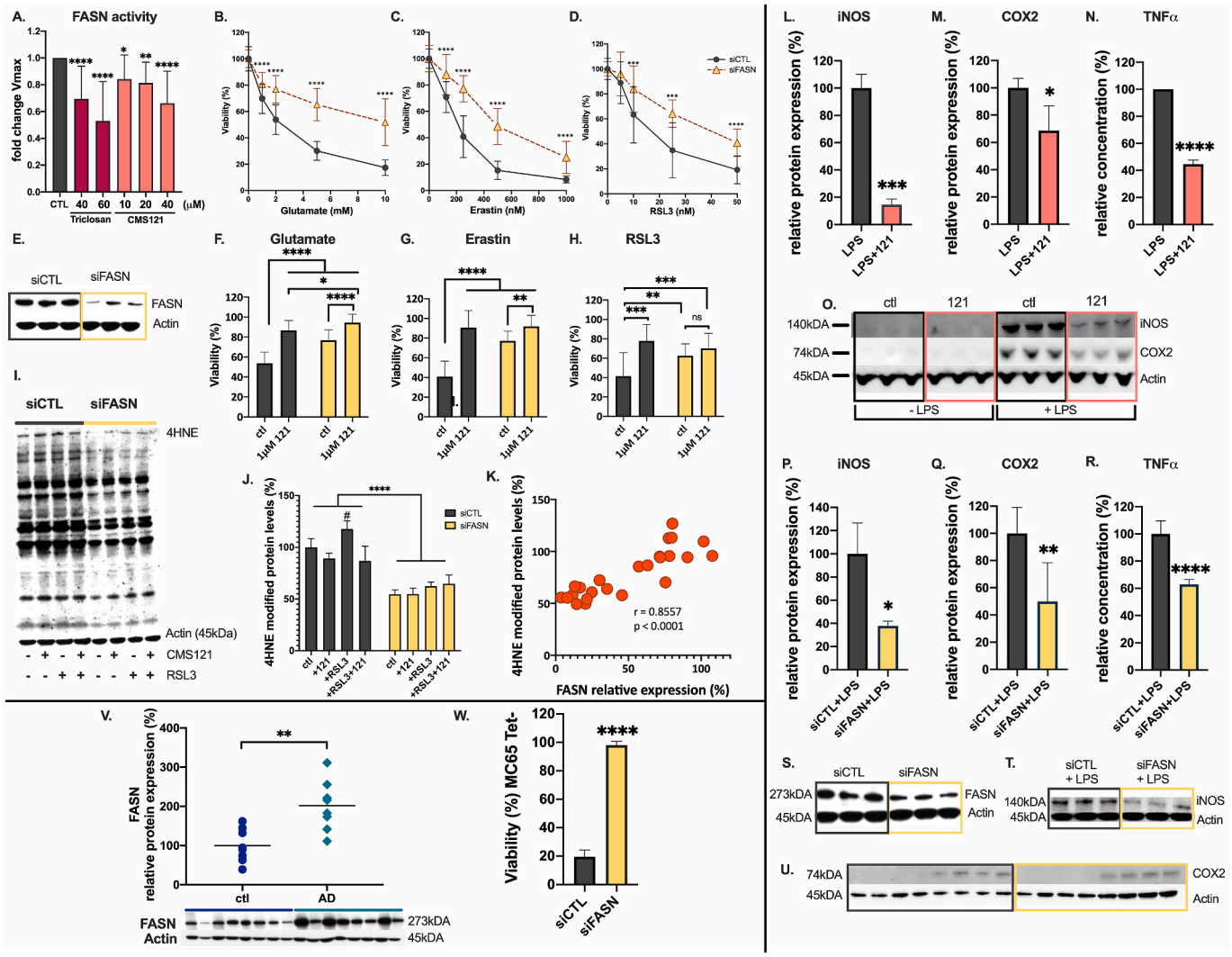

Fig. 5. FASN is a target of CMS121. **A.** CMS121 inhibits the enzymatic activity of FASN measured in HT22 cell lysates in a dose-dependent manner. The Vmax during the linear phase of the kinetic curve decreases with increasing concentrations of CMS121. Triclosan, a known FASN inhibitor was used as a positive control. Fold changes of treatment over vehicle controls are plotted. Results are expressed as mean ± SD. Significance is calculated using one-way ANOVA, the mean of each column was compared with the mean of the control column (N = 18, with 6 independent experiments). *FASN* knockdown (siFASN) of HT22 cells protects against oxytosis/ferroptosis induced by glutamate, erastin and RSL3 (**B-D**). (***q<0.001, ****q<0.0001, multiple T-tests, n = 9 per 3 independent transfections). Transfection efficiency was tested by immunoblotting for FASN (**E**). Exposure of control siRNA (siCTL) transfected HT22 cells to 2 mM glutamate (**F**), 250 nM erastin (**G**) or 25 nM RSL3 (**H**) for 24h leads to ≥50% cell death. 1 μM CMS121, as well as knockdown of *FASN* significantly increased survival rates in all cases. In siFASN-treated cells, 1 μM CMS121 offers additional protection against glutamate and erastin, but not against RSL3 toxicity. Significance is calculated with 2-way ANOVA and Sidak's post-hoc multiple comparisons test (ns = not significant, *p<0.05, **p<0.01, ***p<0.001, ****p<0.0001). **I,J.** 4HNE adduct formation as a measure of lipid peroxidation is decreased in HT22 cells transfected with siRNA against *FASN* (siFASN), compared to control siRNA transfected cells (siCTL) (****p<0.0001, 2-way ANOVA, n = 3). 30min exposure of HT22 cells to RSL3 increases 4HNE adduct formation in siCTL cells (#p<0.05, 2-way ANOVA, Sidak's multiple comparisons test), but not in siFASN transfected cells. In siFASN transfected cells, CMS121 does not have an added protective effect against 4HNE adduct formation. **K.** 4HNE adduct formation correlates significantly with FASN protein expression levels in HT22 cells (r = 0.86, p<0.0001, 2-tailed Pearson correlation, with H_0 stating the absence of association between 4HNE adduct formation and FASN protein levels, n = 6). Both CMS121 **(L–O)** and *FASN* knockdown **(P–U)**, were able to decrease the levels of the inflammatory markers iNOS (**L,P**), COX2 (**M,Q**), and TNFα (**N,R**). Results are expressed as mean ± SD. Significance was calculated using the unpaired T-test (*p<0.05, **p<0.01, ***p<0.001, ****p<0.0001, n = 3–4). Knockdown efficiency of *FASN* in the BV2 microglia was assessed by immunoblotting for FASN (**S**). **V.** In AD patients, protein levels of FASN are significantly increased. Results are expressed as relative protein expression, normalized against human control samples (**p<0.01, unpaired T-test, n = 8). **W.** Knocking down *FASN* protects MC65 cells against intracellular Aβ-induced cell death. Results are expressed as mean ± SD % viability against untreated, Tet + control cells (****p<0.0001, unpaired T-test, n = 3).

despite the presence of antioxidants and the amount of peroxides formed will depend on the amount of peroxidizable substrates such that decreasing their levels might prove to be a more effective approach [44].

One of the most common and toxic by-products of lipid peroxidation is the highly reactive electrophilic aldehyde 4HNE [45]. 4HNE-adducts have been detected in the brains of AD patients at different stages of the disease [5,38] and 4HNE is able to modify the Aβ peptide and facilitate its misfolding and aggregation [46–48]. In our study, 4HNE levels are increased ~50% in the hippocampus of untreated AD mice but treatment with CMS121 reduced 4HNE levels back to WT control levels. Higher levels of lipid peroxidation and inflammation in the AD mice are further supported by the increased protein levels of 15LOX2. 15LOX2 is a member of the LOX enzyme family. Together with COXs and CYPs, LOX enzymes are responsible for the dioxygenation of PUFAs, to generate eicosanoids. These signalling molecules have diverse physiological functions and are important modulators of inflammation, with

both pro- and anti-inflammatory activities. *In vitro*, LOX enzymes play a role in lipid peroxidation and cell death by oxytosis/ferroptosis [10,24,49] and studies show a positive correlation between 15LOX and 4HNE levels [50,51]. In AD, 15LOX2 is increased and it has been argued that this represents a pro-inflammatory state [25]. 15LOX2 levels were normalized in CMS121-treated AD mice. Together with the earlier [34] and new *in vitro* results, as well as the decreased levels of GFAP *in vivo* this suggests that the anti-inflammatory effects of CMS121 are tied to lower levels of lipid peroxidation as measured by 4HNE adduct formation. Electrophiles such as 4HNE are a double-edged sword. At low concentrations 4HNE can activate the antioxidant response via Nrf2 signaling, provoking an "electrophilic counterattack" to oxidative stress. High concentrations, on the other hand, can lead to cytotoxicity [52]. This principle of hormesis has gained much interest in the context of aging and neurodegeneration and is being proposed as an anti-aging molecular mechanism of plant polyphenols like fisetin, the parent compound of CMS121 [53–55]. Our results reinforce this principle as CMS121 too decreases, but does not abolish, lipid peroxidation as a means to protect cells against increased oxidative stress. Similar promising results have been published in a sporadic AD model [56] as well as in diabetes, another disease with an oxidative stress component [57]. Two different chemical entities, gammapyrone [56] and anserine [57], quenched peroxides and restored cellular homeostasis with clear effects on the respective disease phenotypes, *in vivo*.

MC65 cells offer a model to further test the role of lipid peroxides in Aβ toxicity. Indeed, eicosanoids were increased when Aβ production was induced in MC65 neuronal cells. This increase was general and irrespective of the involved enzymatic system (LOX, COX, CYP or even non-enzymatic), the original PUFA (AA, LA or DHA) and the function of the eicosanoid (pro- or anti-inflammatory). We argue that this might be due to a general lipid dysregulation in the *in vitro* AD model. CMS121 treatment led to a general, unselective decrease of these eicosanoids, again indicating a more general effect on lipids. Furthermore, coincident with its effects on eicosanoid levels, CMS121 prevented intracellular Aβ accumulation and cell death in the MC65 cells.

Untargeted metabolomics in mouse cortex and changes in the hippocampal protein levels of FASN confirm key differences in lipid metabolism in the AD mice, with CMS121 normalizing the increased metabolite levels of several groups of lipids, including the group most prone to lipid peroxidation and 4HNE formation, the PUFAs. Other studies have shown more general increased lipid levels in the AD brain [58,59] and the effectiveness of lipid-lowering treatment strategies is being investigated [60,61]. The observed normalization of lipid levels by CMS121 in AD could be explained by increased lipid utilization and/or decreased synthesis. Increased lipid utilization or β-oxidation is reflected by increased levels of carnitines and ketone bodies [62], which we did not observe in the metabolomics results, supporting a possible decrease in lipid synthesis by CMS121 as suggested by the lower palmitate levels after treatment in the AD mice. A further link to a decrease in lipid synthesis was found after DARTS analysis in two distinct cell lines showed that FASN, the enzyme converting malonyl-coA into the lipid precursor palmitate, is a target of CMS121.

Compared to CMS121, gene silencing of *FASN* in neuronal or microglial cell lines showed similar protection against oxytosis/ferroptosis and inflammation. It should be noted that CMS121 does show additional protection in glutamate and erastin-induced oxytosis/ferroptosis, but not in RSL3 induced lipid peroxidation. This is likely due to the fact that CMS121 maintains GSH levels under oxidative stress, *in vitro* [34], thereby preserving the substrate for the lipid peroxidation detoxifier GPX4, whereas *FASN* knockdown is not expected to affect GSH levels in the short term [63]. RSL3, on the other hand inhibits GPX4, inducing lipid peroxidation independently of the GSH levels. Together with the fact that several flavonoids are known FASN inhibitors, our results support the idea of FASN as a target of CMS121. That decreasing lipid levels can lead to a reduction of lipid peroxidation is in line with kinetic models that imply that lipid peroxidation is only weakly dependent on ROS levels but more sensitive to PUFA levels [44].

Interestingly, FASN positive cells are increased in human AD brain, especially around plaques [64] and we found generally increased FASN protein levels in the brains of both AD mice and AD patients. Additionally, *FASN* knockdown protected against Aβ-induced toxicity in human MC65 cells, showing further beneficial effects to targeting FASN in AD. Targeting FASN is also being considered in cancer, fatty liver disease, obesity and type 2 diabetes [65–68], confirming its druggability. And while we show that FASN inhibition protects against oxytosis/ferroptosis, Parisi et al. (2017) showed that the synthesis of fatty acids is activated during necroptosis and FASN inhibition protects against this type of cell death as well. In fact, only the specific inhibition of FASN was protective against necroptosis [69]. With recent research suggesting a role for necroptosis in AD [70], this suggests an additional advantage of inhibiting FASN in AD.

4. Conclusion

The fisetin derivative CMS121 protects against oxytotic/ferroptotic cell death and lipid peroxidation and has anti-inflammatory properties *in vitro*. *In vivo*, CMS121 is able to reduce AD-related cognitive decline in APPswe/PS1ΔE9 transgenic mice and decrease the toxic lipid peroxidation product 4HNE in the mouse hippocampus. We have identified FASN, a key enzyme in the synthesis of lipids which is increased in AD patients, as a target of CMS121. FASN inhibition through CMS121 protects against lipid peroxidation, neuroinflammation and cell death, linking perturbed lipid metabolism to cognitive malfunction, neuroinflammation and neurodegeneration. Even though we did not obtain a baseline cognitive function for the mice in this study, our previous work has shown that 9-month old APP/PSE1 mice already display significant signs of cognitive deficits [12] suggesting that the disease may have begun before the start of the CMS121 treatment. Further study will be required to determine whether CMS121 can indeed reverse any pre-existing pathology. Finally, we also show the benefits of a chemical biology approach to drug discovery in the field of AD: developing a new potential drug against AD and thereby identifying new targets and previously unexplored mechanisms of protection.

5. Methods

5.1. Study design

The objective of this study was to evaluate the effects of CMS121 on memory and cognition in the APPswe/PS1ΔE9 double transgenic mouse model for AD and to ascertain the putative target of CMS121. At 9 months of age, male transgenic mice and controls (C57BL/6J) were fed a diet (Harlan Teklad; Envigo, Indianapolis, USA) with or without 400 ppm CMS121 (leading to an average consumption of 34 mg/kg/day CMS121, based on the measurement of the overall food consumption of the mice housed together in each cage). Treatment lasted for 3 months, followed by behavioral testing and tissue harvesting. Mice (12 per group) were assigned randomly to treatment or control groups and both behavioral testing and data analysis were performed by different blinded researchers. The effect of the compounds in AD was assessed after the 3 months of treatment and any genotype/compound-related changes are defined by comparison to age-matched wild type mice who were fed the control diet. The number of mice per group was determined based on previous experiments [71] and was sufficient to attain statistical power.

5.2. Animals

All animal studies were carried out in accordance with the recommendations in the Guide for the Care and Use of Laboratory Animals of the National Institute of Health. The protocol was approved by the Animal Care and Use Committee of the Salk Institute for Biological Studies. APPswe/PS1ΔE9-transgenic mice express a mouse/human

chimeric APPswe and a mutant human presinilin 1 (PS1ΔE9) on a C57BL/6J genetic background. These mice were previously characterized by Jankowsky et al. [11]. Mouse body weights and food consumption were measured weekly. There were no significant differences between the groups (data not shown). The genotypes were confirmed by PCR according to the Jackson Labs genotyping protocol.

5.3. Human samples

The brain tissue was supplied by Dr. Robert Rissman and Jeffrey Metcalf at the University of California, San Diego (UCSD) Alzheimer's Disease Research Center and the Shiley-Marcos Alzheimer's Disease Research Center. Tissue was obtained from the cortex of eight age and sex-matched (female) control patients and eight AD patients (Table 2). The average age of both groups was 87 years. Control patients had no cognitive complaints with normal neuropsychological test and daily living scores.

5.4. Behavioral assays

A *two-day Morris water maze* to determine spatial memory was performed as described [13]. Briefly, on day one, mice were trained to find the visible platform using cues located around the pool, within a 180s time frame. Four visible platform trials were performed. On day two, 24h after the last visible platform trial, three hidden platform trials were performed. The time it took the mice to find the hidden platform was measured as escape latency. Each trial lasted 180s. The Noldus EthoVision software (Noldus Information Technology, Inc., Leesburg, USA) was used to automatically track and record the mice.

The *elevated plus maze* was used to investigate the presence of a disinhibition phenotype in mice. In an elevated, plus-shaped maze with two open and two enclosed arms, the time mice spent in both types of arms was measured for a total of 5min. Disinhibition was measured by comparing the time spent in the open arms to the time spent in the closed arms. A video-tracking system (Noldus EthoVision) was used to automatically collect the behavioral data [13].

Contextual memory, which requires a functioning hippocampus, was tested using a *fear conditioning* paradigm as described [13]. Fear conditioning chambers from Med Associates Inc. with Video Freeze Software (Med Associates Inc, St. Albans, VT, USA) were used. On day one mice were trained by allowing them to explore the chamber for 120s, they were then presented with a 30s tone (2 kHz; 85 dB intensity) immediately followed by a foot shock (0.7 mA, 2s). The tone/shock pairing was repeated after 30s and mice were again allowed to explore the chamber for 120s before removing them. On day two, the contextual memory of the mice was tested by placing them again in the chambers for the same amount of time but without the tone or the shock and measuring their freezing time. The mouse will freeze if it remembers and associates that environment with the aversive stimulus.

5.5. Western blot

Hippocampal tissue samples or cell lysates were homogenized in ten volumes of RIPA lysis buffer (50 mM Tris, pH7.5, 150 mM sodium chloride, 0.1% sodium dodecyl sulfate and 0.5% deoxycholate, and 1% NP40) containing a cocktail of protease and phosphatase inhibitors (20 mg/ml each of pepstatin A, aprotinin, phosphoramidon, and leupeptin; 0.5 mM 4-(2-aminoethyl) benzenesulfonyl fluoride hydrochloride; 1 mM EGTA; 5 mM fenvalerate; and 5 mM cantharidin). Samples were sonicated (2 × 10s) and centrifuged at 100,000×*g* for 60 min at 4 °C. Protein concentrations in the cell extracts were determined using a bicinchoninic acid protein assay (Pierce™, Thermo Fisher Scientific). Equal amounts of protein were solubilized in 2.5x SDS-sample buffer, separated on 4–12% SDS-polyacrylamide gradient gels, transferred to a nitrocellulose membrane (0.45 μM, Bio-Rad) via semi-dry transfer (Trans-Blot® Turbo (Bio-Rad) and immunoblotted with the respective antibodies (4HNE 1/500 EDM Millipore #5605; 15LOX2 1/1000 Cayman chemical #10004454; 6E10 1/1000 Biolegend SIG-39320; COX2 1/1000 Cell Signaling Technology #12282; FASN 1/1000 Cell Signaling Technology #3189; GFAP 1/1000 EMD Millipore #MAB3402; iNOS 1/1000 Cell Signaling Technology #13120). Levels of the protein of interest were normalized to actin (1/20000 Cell Signaling Technology #5125). Relative protein expression levels were calculated using QuantityOne software (Bio-Rad) and by comparing to the untreated WT mice. To measure the level of 4HNE protein adducts, the optical density of the entire lane was determined (the whole lane was considered as a single band) and normalized against the respective actin levels.

5.6. Metabolomics

Untargeted metabolomics was performed by Metabolon® on mouse cortex. Mouse cortex was snap frozen after isolation and stored at −80

Table 2
Demographics of individuals used for protein analysis.

Case Number	Diagnosis	Age	Sex	PM (h)	APOE	Braak	BT	MMSE
1 × 5070	Control	97	F	12	3/3	1	2	26
2 × 5302	Control	83	F	72	2/4	1		29
3 × 5512	Control	89	F	12	2/3	2		30
4 × 5049	Control	102	F	9	3/3	1		27
5 × 4870	Control	63	F	8	3/3	1	0	30
6 × 4689	Control	79	F	6	3/3	0	1	27
7 × 5248	Control	93	F	18	3/3	1		30
8 × 5447	Control	91	F	8	3/3	1		28
9 × 5759	AD	87	F	18	3/3	6	9	18
10 × 5798	AD	87	F	7	3/3	5	3	11
11 × 5799	AD	82	F	15		6	26	9
12 × 5764	AD	82	F	8	3/4	6	33	23
13 × 5763	AD	94	F	24	3/4	5	25	13
14 × 5792	AD	93	F	10	3/3	5	8	22
15 × 5761	AD	89	F		3/4	5	3	25
16 × 5755	AD	83	F	12	4/4	6	18	19

PM: time of tissue harvesting post-mortem.
APOE: genotyping results for ApoE2 (2), ApoE3 (3) and ApoE4 (4).
BT: Blessed test results for cognitive impairment [72] with scores ranging from 0 (no impairment) to 33 (severe impairment). Scores were not available for 5 control subjects.
Braak staging marks the disease propagation with respect to the location of the tangle-bearing neurons and the severity of changes with 1–2: clinically silent cases; 3–4: incipient Alzheimer's disease; 5–6: fully developed Alzheimer's disease [73].
MMSE: Mini-Mental State Examination, a score of 20–24 suggests mild dementia, 13–20 suggests moderate and <12 implies severe dementia.

°C until further processing. Samples were prepared using the automated MicroLab STAR® system from Hamilton Company. A recovery standard was added prior to the first step in the extraction process for QC purposes. Proteins were precipitated with methanol under vigorous shaking for 2min (Glen Mills GenoGrinder 2000) followed by centrifugation. The resulting extract was divided into different fractions: one for analysis by UPLC-MS/MS with positive ion mode electrospray ionization, one for analysis by UPLC-MS/MS with negative ion mode electrospray ionization, one for analysis by GC-MS. Raw data was extracted, peak-identified and QC processed using Metabolon's hardware and software. Compounds were identified by comparison to library entries of purified standards or recurrent unknown entities. Metabolon maintains a library based on authenticated standards that contains the retention time/index (RI), mass to charge ratio (*m/z*), and chromatographic data (including MS/MS spectral data) on all molecules present in the library. Peaks were quantified using area-under-the-curve.

5.7. Cell cultures

The HT22 mouse hippocampal neuronal cell line and HeLa cells are propagated in regular DMEM. BV2 microglial cells were propagated in low glucose DMEM. Culture medium was supplemented with 10% FBS. Cells were passed every 3 days or at approximately 80% confluence. MC65 cells were propagated in regular DMEM supplemented with 1 μM Tet to suppress the formation of intracellular Aβ.

5.8. In vitro lipid peroxidation

Cells were seeded onto 96-well black walled microtiter plates at a density of 2×10^4 cells/well. The next day, cells were treated with 1 μM CMS121 alone or in the presence of RSL3 (250 nM) or LPS (25 ng/ml), for 4h and 24h respectively. The medium was then replaced with 100 μl loading medium (phenol red-free Hank's balanced salt solution containing 2 μM Bodipy 581/591 (Invitrogen, D3861)). After 30min, fluorescence was determined (λ excitation = 530 nm, λ emission = 590 nm for unoxidized and λ excitation = 485 nm, λ emission = 528 nm for oxidized) using a microplate reader (Molecular Devices). The fluorescence was normalized to untreated control cells. The experiments were done 3–4 times and each treatment within each experiment was done in sextuplicate.

5.9. Intracellular Aβ-accumulation and cell death

MC65 cells were plated at a density of 5×10^5 cells/dish in 35 mm culture dishes and grown for 24h. The next day the cells were put into OptiMEM (Invitrogen) with or without Tet for the various experimental paradigms. Aβ aggregates were measured by immunoblotting with the 6E10 antibody (6E10 1/1000, Biolegend, SIG-39320). Cell death was determined using the 3-(4,5-dimethylthiazol-2-yl)-2,5-diphenyltetrazolium bromide (MTT) test [74].

5.10. Eicosanoid analysis

Eicosanoids were measured in the supernatants of Tet+ and Tet- MC65 cells, by the University of California San Diego (UCSD) Lipidomics Core. The protocol was based on Currais et al. [12] and Quehenberger et al. [75]. Briefly, the eicosanoids were separated by reverse-phase chromatography using a 1.7 μM 2.1 × 100 mm BEH Shield Column (Waters, Milford, MA, USA) and an Acquity UPLC system (Waters). The column was equilibrated with buffer A, consisting of 60/40/0.02 water/acetonitrile/acetic acid = 60/40/0.02 (v/v/v). 5 μl of sample was injected via the autosampler. Samples were eluted with a step gradient to 100% buffer B consisting of acetonitrile/isopropanol = 50/50(v/v). The liquid chromatography effluent was interfaced with a mass spectrometer, and mass spectral analysis was performed on an AB SCIEX 6500 QTrap mass spectrometer equipped with an IonDrive Turbo V source (AB SCIEX, Framingham, MA, USA). Eicosanoids were measured using multiple reaction monitoring (MRM) pairs with the instrument operating in the negative ion mode. Collisional activation of the eicosanoid precursor ions was achieved with nitrogen as the collision gas, and the eicosanoids were identified by matching their MRM signal and chromatographic retention time with those of pure identical standards. Eicosanoids were quantified by the stable isotope dilution method: identical amounts of deuterated internal standards were added to each sample and to all the primary standards used to generate standard curves. To calculate the levels of eicosanoids in a sample, ratios of peak areas between endogenous eicosanoids and matching deuterated internal eicosanoids were calculated. Ratios were converted to absolute amounts by linear regression analysis of standard curves generated under identical conditions [12,75]. Results are presented as fold changes against control cells (untreated Tet + cells). Currently, the UCSD Lipidomics Core can quantify over 150 eicosanoids at sub-fmole levels.

5.11. Drug affinity responsive target stability

Drug affinity responsive target stability (DARTS) was performed based on Goldberg et al. [33] and Pai et al. [76]. Briefly, untreated HT22 and HeLa cells were lysed with M-PER (Pierce, 78503) supplemented with protease and phosphatase inhibitors (Roche, 11697498001 and 4906845001). Lysates were cleared at 14000RPM for 15min. Supernatants were adjusted with M-PER to equivalent protein levels and treated with vehicle control or 5, 10, 25, 50 and 100 μM CMS121 for 60min. Samples were then digested with Pronase (Roche, 10165921001) for 30 min at room temperature and separated by SDS-PAGE. To identify unique bands in CMS121 treated samples - these represent putative targets of CSM121 spared from proteolysis - proteins were visualized by Coomassie blue staining. These lanes were then excised, trypsin-digested and subjected to mass spectrometry [33,76]. Scaffold™ Proteome software was used to identify the proteins of interest. Proteins considered of significance had more than 100 spectral counts after treatment with CMS121 and showed at least a 2-fold enrichment in the CMS121 treated samples, compared to vehicle controls, in both cell lines.

5.12. Fatty acid synthase enzymatic activity assay

HT22 cells were plated in 10 cm dishes. At approximately 80% confluency, cells were rinsed twice and collected with ice cold PBS using a cell scraper. After centrifugation, cells were resuspended in assay buffer (0.1 M KH_2PO_4, 1 mM EDTA, pH7.0). Cells were lysed by applying one freeze-thaw cycle, followed by gentle sonication. The activity of FASN was determined by monitoring the decrease of NADPH absorbance over a time period of 30 min at 340 nm in the presence of acetyl-CoA (25 μM) and malonyl-CoA (100 μM) at 37 °C on HT22 cell lysates. Triclosan was used as a positive control [77]. Vmax was calculated in the linear range of the kinetic curve and compared to the Vmax of the vehicle control (no substrate).

5.13. Cell transfections

Cells were seeded in 60 mm dishes at a density of 5×10^4 cells/ml. 24h post-seeding, cells were transfected with siRNA against fatty acid synthase (FASN, Santa Cruz, SC-41516, 17 pmol), using lipofectamine (RNAiMAX, ThermoFisher) as the transfection reagent and Opti-MEM™ (Gibco™) as the transfection medium. Control siRNA (Qiagen, 1027280) was used as a negative control. Cells were harvested 24h post-transfection and seeded into appropriate dishes for further study. Transfection efficiency was determined via immunoblotting against FASN (1/1000, Cell Signaling Technology, #3189).

5.14. In vitro oxytosis/ferroptosis

HT22 cells were plated in 96-well plates at a density of 3×10^4 cells/

ml. 24h post seeding, cells were exposed to different concentration of glutamate (0–10 mM), erastin (0–1 μM) and RSL3 (0–50 nM) to induce oxytosis/ferroptosis. All 3 compounds are known inducers of oxytosis/ferroptosis [10]. The MTT test was used to assess cell viability 24h post exposure [74].

5.15. In vitro inflammation

BV2 microglial cells were seeded at a density of 1×10^5 cells/ml in low glucose DMEM in 35 mm dishes. On the following day, culture medium was replaced by high glucose DMEM. Inflammation was induced by adding 25 ng/ml bacterial lipopolysaccharide (LPS) to the culture medium. Cell culture supernatants and cell pellets were collected 24h post-exposure for further analysis. The supernatants were briefly centrifuged to remove cell debris. TNFα was determined using an ELISA kit (R&D Systems, SMTA00B), according to the manufacturer's instructions. TNFα concentrations were normalized against protein content as determined on the cell pellets using the BCA assay (Pierce, 23225). Relative protein expression of iNOS (1/1000, Cell Signaling Technology, #13120) and COX2 (1/1000, Cell Signaling Technology, #12282) were determined by immunoblotting as additional indicators of inflammation.

5.16. Quantification and statistical analysis

Statistical analysis was performed using GraphPad Prism 8 and a p-value of <0.05 was considered as significant. The data representation and statistical test applied, including the number of replicates, is described in the figure legends.

Declaration of competing interest

The authors declare that they have no known competing financial interests or personal relationships that could have appeared to influence the work reported in this paper.

Acknowledgements and funding information

This study was supported by grants from the Shiley Foundation (GA, JG), National Institutes of Health (RO1 AG046153, RF1 AG054714 and R41 AI104034 to PM), and the Edward N. & Della Thome Memorial Foundation (PM) and the Shiley-Marcos Alzheimer's Disease Research Center at University of California San Diego (UCSD) (AC). We thank Dr. David Schubert (Salk Institute) for his insightful comments and critical revision of the manuscript, Dr. Oswald Quehenberger (UCSD) for his advice and support regarding the eicosanoid analyses and Dr. Robert Riessman and Jeffrey Metcalf from the UCSD Alzheimer's Disease Research Center and the Shiley-Marcos Alzheimer's Disease Research Center for providing the human tissue.

Appendix A. Supplementary data

Supplementary data to this article can be found online at https://doi.org/10.1016/j.redox.2020.101648.

References

[1] C.A. Lane, J. Hardy, J.M. Schott, Alzheimer's disease, Eur. J. Neurol. 25 (2018) 59–70, https://doi.org/10.1111/ene.13439.
[2] L.S. Schneider, F. Mangialasche, N. Andreasen, H. Feldman, E. Giacobini, R. Jones, et al., Clinical trials and late-stage drug development for Alzheimer's disease: an appraisal from 1984 to 2014, J. Intern. Med. 275 (2014) 251–283, https://doi.org/10.1111/joim.12191.
[3] A. Ashraf, J. Jeandriens, H.G. Parkes, P.-W. So, Iron dyshomeostasis, lipid peroxidation and perturbed expression of cystine/glutamate antiporter in Alzheimer's disease: evidence of ferroptosis, Redox Biol 32 (2020) 101494, https://doi.org/10.1016/J.REDOX.2020.101494.
[4] K. Trares, X. Gào, L. Perna, D. Rujescu, H. Stocker, T. Möllers, et al., Associations of urinary 8-iso-prostaglandin F2α levels with all-cause dementia, Alzheimer's disease, and vascular dementia incidence: results from a prospective cohort study, Alzheimers Dement 16 (5) (2020) 804–813, https://doi.org/10.1002/alz.12081.
[5] M.A. Bradley, W.R. Markesbery, M.A. Lovell, Increased levels of 4-hydroxynonenal and acrolein in the brain in preclinical Alzheimer disease, Free Radic. Biol. Med. 48 (2010) 1570–1576, https://doi.org/10.1016/j.freeradbiomed.2010.02.016.
[6] M.A. Bradley-Whitman, M.A. Lovell, Biomarkers of lipid peroxidation in Alzheimer disease (AD): an update, Arch. Toxicol. 89 (2015) 1035–1044, https://doi.org/10.1007/s00204-015-1517-6.
[7] M. Prior, C. Chiruta, A. Currais, J. Goldberg, J. Ramsey, R. Dargusch, et al., Back to the future with phenotypic screening, ACS Chem. Neurosci. 5 (2014) 503–513, https://doi.org/10.1021/cn500051h.
[8] S. Tan, D. Schubert, P. Maher, Oxytosis: a novel form of programmed cell death, Curr. Top. Med. Chem. 1 (2001) 497–506.
[9] S.J. Dixon, K.M. Lemberg, M.R. Lamprecht, R. Skouta, E.M. Zaitsev, C.E. Gleason, et al., Ferroptosis: an iron-dependent form of non-apoptotic cell death, Cell 149 (2012) 1060–1072, https://doi.org/10.1016/J.CELL.2012.03.042.
[10] J. Lewerenz, G. Ates, A. Methner, M. Conrad, P. Maher, Oxytosis/ferroptosis-(Re-) emerging roles for oxidative stress-dependent non-apoptotic cell death in diseases of the central nervous system, Front. Neurosci. 12 (2018) 214, https://doi.org/10.3389/fnins.2018.00214.
[11] J.L. Jankowsky, D.J. Fadale, J. Anderson, G.M. Xu, V. Gonzales, N.A. Jenkins, et al., Mutant presenilins specifically elevate the levels of the 42 residue β-amyloid peptide in vivo: evidence for augmentation of a 42-specific γ secretase, Hum. Mol. Genet. 13 (2004) 159–170, https://doi.org/10.1093/hmg/ddh019.
[12] A. Currais, M. Prior, R. Dargusch, A. Armando, J. Ehren, D. Schubert, et al., Modulation of p25 and inflammatory pathways by fisetin maintains cognitive function in Alzheimer's disease transgenic mice, Aging Cell 13 (2014) 379–390, https://doi.org/10.1111/acel.12185.
[13] M. Prior, R. Dargusch, J.L. Ehren, C. Chiruta, D. Schubert, The neurotrophic compound J147 reverses cognitive impairment in aged Alzheimer's disease mice, Alzheimer's Res. Ther. 5 (2013) 25, https://doi.org/10.1186/alzrt179.
[14] E. Finger, J. Zhang, B. Dickerson, Y. Bureau, M. Masellis, Alzheimer's disease neuroimaging initiative. Disinhibition in alzheimer's disease is associated with reduced right frontal Pole cortical thickness, J Alzheimers Dis 60 (2017) 1161–1170, https://doi.org/10.3233/JAD-170348.
[15] M.M. Gaschler, B.R. Stockwell, Lipid peroxidation in cell death, Biochem. Biophys. Res. Commun. 482 (2017) 419–425, https://doi.org/10.1016/j.bbrc.2016.10.086.
[16] R. Sultana, M. Perluigi, D.A. Butterfield, Lipid peroxidation triggers neurodegeneration: a redox proteomics view into the Alzheimer disease brain, Free Radic. Biol. Med. 62 (2013) 157–169, https://doi.org/10.1016/j.freeradbiomed.2012.09.027.
[17] U.C.S. Yadav, K.V. Ramana, Regulation of NF-κB-induced inflammatory signaling by lipid peroxidation-derived aldehydes, Oxid Med Cell Longev 2013 (2013) 690545, https://doi.org/10.1155/2013/690545.
[18] M. Breitzig, C. Bhimineni, R. Lockey, N. Kolliputi, 4-Hydroxy-2-nonenal: a critical target in oxidative stress? Am. J. Physiol. Cell Physiol. 311 (2016) C537–C543, https://doi.org/10.1152/ajpcell.00101.2016.
[19] K. Uchida, HNE as an inducer of COX-2, Free Radic. Biol. Med. 111 (2017) 169–172, https://doi.org/10.1016/j.freeradbiomed.2017.02.004.
[20] A. Ayala, M.F. Muñoz, S. Argüelles, Lipid peroxidation: production, metabolism, and signaling mechanisms of malondialdehyde and 4-hydroxy-2-nonenal, Oxid Med Cell Longev 2014 (2014) 360438, https://doi.org/10.1155/2014/360438.
[21] H. Kuhn, S. Banthiya, K. Van Leyen, Mammalian lipoxygenases and their biological relevance, Biochim. Biophys. Acta Mol. Cell Biol. Lipids 1851 (2015) 308–330, https://doi.org/10.1016/j.bbalip.2014.10.002.
[22] W.S. Yang, K.J. Kim, M.M. Gaschler, M. Patel, M.S. Shchepinov, B.R. Stockwell, Peroxidation of polyunsaturated fatty acids by lipoxygenases drives ferroptosis, Proc. Natl. Acad. Sci. U. S. A. 113 (2016) e4966–e4975, https://doi.org/10.1073/pnas.1603244113.
[23] A. Seiler, M. Schneider, H. Förster, S. Roth, E.K. Wirth, C. Culmsee, et al., Glutathione peroxidase 4 senses and translates oxidative stress into 12/15-lipoxygenase dependent- and AIF-mediated cell death, Cell Metabol. 8 (2008) 237–248, https://doi.org/10.1016/j.cmet.2008.07.005.
[24] S.E. Wenzel, Y.Y. Tyurina, J. Zhao, C.M. St Croix, H.H. Dar, G. Mao, et al., PEBP1 wardens ferroptosis by enabling lipoxygenase generation of lipid death signals, Cell 171 (2017) 628–641, e26.
[25] X. Wang, M. Zhu, E. Hjorth, V. Cortés-Toro, H. Eyjolfsdottir, C. Graff, et al., Resolution of inflammation is altered in Alzheimer's disease, Alzheimers Dement 11 (2015) 40–50, https://doi.org/10.1016/j.jalz.2013.12.024, e1-2.
[26] J.A. Oostveen, E. Dunn, D.B. Carter, E.D. Hall, Neuroprotective efficacy and mechanisms of novel pyrrolopyrimidine lipid peroxidation inhibitors in the gerbil forebrain ischemia model, J. Cerebr. Blood Flow Metabol. 18 (1998) 539–547, https://doi.org/10.1097/00004647-199805000-00009.
[27] A. Currais, O. Quehenberger, A.M. Armando, D. Daugherty, P. Maher, D. Schubert, Amyloid proteotoxicity initiates an inflammatory response blocked by cannabinoids, Npj Aging Mech Dis 2 (2016) 16012, https://doi.org/10.1038/npjamd.2016.12.
[28] X. Wei, H. Song, L. Yin, M.G. Rizzo, R. Sidhu, D.F. Covey, et al., Fatty acid synthesis configures the plasma membrane for inflammation in diabetes, Nature 539 (2016) 294–298, https://doi.org/10.1038/nature20117.
[29] R.G. Carroll, Z. Zasłona, S. Galván-peña, E.L. Koppe, C. Sévin, S. Angiari, et al., An unexpected link between fatty acid synthase and cholesterol synthesis in proinflammatory macrophage activation, J. Biol. Chem. 293 (2018) 5509–5521, https://doi.org/10.1074/jbc.RA118.001921.

[30] C. Zhang, Y. Wang, D. Wang, J. Zhang, F. Zhang, NSAID exposure and risk of alzheimer's disease: an updated meta-analysis from cohort studies, Front. Aging Neurosci. 10 (2018), https://doi.org/10.3389/FNAGI.2018.00083.

[31] B. Decourt, D. Lahiri, M. Sabbagh, Targeting tumor necrosis factor Alpha for alzheimer's disease, Curr. Alzheimer Res. 13 (2016), https://doi.org/10.2174/1567205013666160930110551, 1–1.

[32] D.Y. Lee, C.J. Hwang, J.Y. Choi, M.H. Park, M.J. Song, K.W. Oh, et al., KRICT-9 inhibits neuroinflammation, amyloidogenesis and memory loss in Alzheimer's disease models, Oncotarget 8 (2017) 68654–68667, https://doi.org/10.18632/oncotarget.19818.

[33] J. Goldberg, A. Currais, M. Prior, W. Fischer, C. Chiruta, E. Ratliff, et al., The mitochondrial ATP synthase is a shared drug target for aging and dementia, Aging Cell 17 (2018), e12715, https://doi.org/10.1111/acel.12715.

[34] C. Chiruta, D. Schubert, R. Dargusch, P. Maher, Chemical modification of the multi-target neuroprotective compound fisetin, J. Med. Chem. 55 (2012) 378–389, https://doi.org/10.1021/JM2012563.

[35] A. Currais, L. Huang, J. Goldberg, M. Petrascheck, G. Ates, A. Pinto-Duarte, et al., Elevating acetyl-CoA levels reduces aspects of brain aging, Elife 8 (2019), e47866, https://doi.org/10.7554/eLife.47866.

[36] M. Perluigi, R. Coccia, D.A. Butterfield, 4-Hydroxy-2-nonenal, a reactive product of lipid peroxidation, and neurodegenerative diseases: a toxic combination illuminated by redox proteomics studies, Antioxidants Redox Signal. 17 (2012) 1590–1609, https://doi.org/10.1089/ars.2011.4406.

[37] R. Sultana, M. Perluigi, D.A. Butterfield, Protein oxidation and lipid peroxidation in brain of subjects with alzheimer's disease: insights into mechanism of neurodegeneration from redox proteomics, Antioxidants Redox Signal. 8 (2006) 2021–2037, https://doi.org/10.1089/ars.2006.8.2021.

[38] T.T. Reed, W.M. Pierce, W.R. Markesbery, D.A. Butterfield, Proteomic identification of HNE-bound proteins in early Alzheimer disease: insights into the role of lipid peroxidation in the progression of AD, Brain Res. 1274 (2009) 66–76, https://doi.org/10.1016/j.brainres.2009.04.009.

[39] M. Fukuda, F. Kanou, N. Shimada, M. Sawabe, Y. Saito, S. Murayama, et al., Elevated levels of 4-hydroxynonenal-histidine Michael adduct in the hippocampi of patients with Alzheimer's disease, Biomed. Res. 30 (2009) 227–233, https://doi.org/10.2220/biomedres.30.227.

[40] X. Zhu, R.J. Castellani, P.I. Moreira, G. Aliev, J.C. Shenk, S.L. Siedlak, et al., Hydroxynonenal-generated crosslinking fluorophore accumulation in Alzheimer disease reveals a dichotomy of protein turnover, Free Radic. Biol. Med. 52 (2012) 699–704, https://doi.org/10.1016/j.freeradbiomed.2011.11.004.

[41] N. Benseny-Cases, O. Klementieva, M. Cotte, I. Ferrer, J. Cladera, Microspectroscopy (μFTIR) reveals co-localization of lipid oxidation and amyloid plaques in human Alzheimer disease brains, Anal. Chem. 86 (2014) 12047–12054, https://doi.org/10.1021/ac502667b.

[42] S.W. Scheff, M.A. Ansari, E.J. Mufson, Oxidative stress and hippocampal synaptic protein levels in elderly cognitively intact individuals with Alzheimer's disease pathology, Neurobiol. Aging 42 (2016) 1–12, https://doi.org/10.1016/J.NEUROBIOLAGING.2016.02.030.

[43] S. Arlt, T. Müller-Thomsen, U. Beisiegel, A. Kontush, Effect of one-year vitamin C- and E-supplementation on cerebrospinal fluid oxidation parameters and clinical course in alzheimer's disease, Neurochem. Res. 37 (2012) 2706–2714, https://doi.org/10.1007/s11064-012-0860-8.

[44] P. Zimniak, Relationship of electrophilic stress to aging, Free Radic. Biol. Med. 51 (2011) 1087–1105, https://doi.org/10.1016/j.freeradbiomed.2011.05.039.

[45] M. Shoeb, N.H. Ansari, S.K. Srivastava, K.V. Ramana, 4-Hydroxynonenal in the pathogenesis and progression of human diseases, Curr. Med. Chem. 21 (2014) 230–237, https://doi.org/10.2174/09298673113209990181.

[46] L. Liu, H. Komatsu, I.V.J. Murray, P.H. Axelsen, Promotion of amyloid β protein misfolding and fibrillogenesis by a lipid oxidation product, J. Mol. Biol. 377 (2008) 1236–1250, https://doi.org/10.1016/j.jmb.2008.01.057.

[47] J.A.N. Bieschke, Q. Zhang, D.A. Bosco, R.A. Lerner, E.T. Powers, P. Wentworth, et al., Small molecule oxidation products trigger disease-associated protein misfolding, Acc. Chem. Res. 39 (2006) 611–619, https://doi.org/10.1021/ar0500766.

[48] D.A. Butterfield, M.L. Bader Lange, R. Sultana, Involvements of the lipid peroxidation product, HNE, in the pathogenesis and progression of Alzheimer's disease, Biochim. Biophys. Acta Mol. Cell Biol. Lipids 1801 (2010) 924–929, https://doi.org/10.1016/j.bbalip.2010.02.005.

[49] Y. Li, P. Maher, D. Schubert, A role for 12-lipoxygenase in nerve cell death caused by glutathione depletion, Neuron 19 (1997) 453–463, https://doi.org/10.1016/s0896-6273(00)80953-8.

[50] W. Zhang, W. Zhong, Q. Sun, X. Sun, Z. Zhou, Hepatic overproduction of 13-HODE due to ALOX15 upregulation contributes to alcohol-induced liver injury in mice, Sci. Rep. 7 (2017) 8976, https://doi.org/10.1038/s41598-017-02759-0.

[51] E.G. Bromfield, B.P. Mihalas, M.D. Dun, R. John Aitken, E.A. McLaughlin, J.L. H. Walters, et al., Inhibition of arachidonate 15-lipoxygenase prevents 4-hydroxynonenal-induced protein damage in male germ cells, Biol. Reprod. 96 (2017) 598–609, https://doi.org/10.1093/biolre/iox005.

[52] A. Gęgotek, E. Skrzydlewska, Biological effect of protein modifications by lipid peroxidation products, Chem. Phys. Lipids 221 (2019) 46–52, https://doi.org/10.1016/j.chemphyslip.2019.03.011.

[53] V. Calabrese, C. Cornelius, S. Cuzzocrea, I. Iavicoli, E. Rizzarelli, E. Calabrese, Hormesis, cellular stress response and vitagenes as critical determinants in aging and longevity, Mol. Aspect. Med. 32 (2011) 279–304, https://doi.org/10.1016/J.MAM.2011.10.007.

[54] S. Miquel, C. Champ, J. Day, E. Aarts, B.A. Bahr, M. Bakker, et al., Poor cognitive ageing: vulnerabilities, mechanisms and the impact of nutritional interventions, Ageing Res. Rev. 42 (2018) 40–55, https://doi.org/10.1016/J.ARR.2017.12.004.

[55] M. Leri, M. Scuto, M.L. Ontario, V. Calabrese, E.J. Calabrese, M. Bucciantini, et al., Healthy effects of plant polyphenols: molecular mechanisms, Int. J. Mol. Sci. 21 (2020) 1250, https://doi.org/10.3390/ijms21041250.

[56] V. Pilipenko, K. Narbute, I. Amara, A. Trovato, M. Scuto, J. Pupure, et al., GABA-containing compound gammapyrone protects against brain impairments in Alzheimer's disease model male rats and prevents mitochondrial dysfunction in cell culture, J. Neurosci. Res. 97 (2019) 708–726, https://doi.org/10.1002/jnr.24396.

[57] V. Peters, V. Calabrese, E. Forsberg, N. Volk, T. Fleming, H. Baelde, et al., Protective actions of anserine under diabetic conditions, Int. J. Mol. Sci. 19 (2018) 2751, https://doi.org/10.3390/ijms19092751.

[58] M.L. Nasaruddin, C. Hölscher, P. Kehoe, S.F. Graham, B.D. Green, Wide-ranging alterations in the brain fatty acid complement of subjects with late Alzheimer's disease as detected by GC-MS, Am J Transl Res 8 (2016) 154–165.

[59] V.R. Varma, A.M. Oommen, S. Varma, R. Casanova, Y. An, R.M. Andrews, et al., Brain and blood metabolite signatures of pathology and progression in Alzheimer disease: a targeted metabolomics study, PLoS Med. 15 (2018), e1002482, https://doi.org/10.1371/journal.pmed.1002482.

[60] C. Reitz, Dyslipidemia and the risk of Alzheimer's disease, Curr. Atherosclerosis Rep. 15 (2013) 307, https://doi.org/10.1007/s11883-012-0307-3.

[61] B.G. Schultz, D.K. Patten, D.J. Berlau, The role of statins in both cognitive impairment and protection against dementia: a tale of two mechanisms, Transl. Neurodegener. 7 (2018) 5, https://doi.org/10.1186/s40035-018-0110-3.

[62] D. Daugherty, J. Goldberg, W. Fischer, R. Dargusch, P. Maher, D. Schubert, A novel Alzheimer's disease drug candidate targeting inflammation and fatty acid metabolism, Alzheimer's Res. Ther. 9 (2017) 50, https://doi.org/10.1186/s13195-017-0277-3.

[63] G. Cheng, A.P. Palanisamy, Z.P. Evans, A.G. Sutter, L. Jin, I. Singh, et al., Cerulenin blockade of fatty acid synthase reverses hepatic steatosis in ob/ob mice, PloS One 8 (2013), e75980, https://doi.org/10.1371/journal.pone.0075980.

[64] R. Thangavel, D. Kempuraj, S. Zaheer, S. Raikwar, M.E. Ahmed, G.P. Selvakumar, et al., Glia maturation factor and mitochondrial uncoupling proteins 2 and 4 expression in the temporal cortex of alzheimer's disease brain, Front. Aging Neurosci. 9 (2017) 150, https://doi.org/10.3389/fnagi.2017.00150.

[65] J.A. Menendez, R. Lupu, Fatty acid synthase (FASN) as a therapeutic target in breast cancer, Expert Opin. Ther. Targets 21 (2017) 1001–1016, https://doi.org/10.1080/14728222.2017.1381087.

[66] Y. Yoshii, T. Furukawa, N. Oyama, Y. Hasegawa, Y. Kiyono, R. Nishii, et al., Fatty acid synthase is a key target in multiple essential tumor functions of prostate cancer: uptake of radiolabeled acetate as a predictor of the targeted therapy outcome, PloS One 8 (2013), e64570, https://doi.org/10.1371/journal.pone.0064570.

[67] T.S. Angeles, R.L. Hudkins, Recent advances in targeting the fatty acid biosynthetic pathway using fatty acid synthase inhibitors, Expet Opin. Drug Discov. 11 (2016) 1187–1199, https://doi.org/10.1080/17460441.2016.1245286.

[68] D. Buckley, G. Duke, T.S. Heuer, M. O'Farrell, A.S. Wagman, W. McCulloch, et al., Fatty acid synthase – modern tumor cell biology insights into a classical oncology target, Pharmacol. Ther. 177 (2017) 23–31, https://doi.org/10.1016/J.PHARMTHERA.2017.02.021.

[69] L.R. Parisi, N. Li, G.E. Atilla-Gokcumen, Very long chain fatty acids are functionally involved in necroptosis, Cell Chem Biol 24 (2017) 1445–1454, https://doi.org/10.1016/j.chembiol.2017.08.026, e8.

[70] A. Caccamo, C. Branca, I.S. Piras, E. Ferreira, M.J. Huentelman, W.S. Liang, et al., Necroptosis activation in Alzheimer's disease, Nat. Neurosci. 20 (2017) 1236–1246, https://doi.org/10.1038/nn.4608.

[71] A. Currais, J. Goldberg, C. Farrokhi, M. Chang, M. Prior, R. Dargusch, et al., A comprehensive multiomics approach toward understanding the relationship between aging and dementia, Aging (Albany NY) 7 (2015) 937–955, https://doi.org/10.18632/aging.100838.

[72] G. Blessed, B.E. Tomlinson, M. Roth, The association between quantitative measures of dementia and of senile change in the cerebral grey matter of elderly subjects, Br. J. Psychiatry 114 (1968) 797–811, https://doi.org/10.1192/bjp.114.512.797.

[73] H. Braak, E. Braak, Staging of alzheimer's disease-related neurofibrillary changes, Neurobiol. Aging 16 (1995) 271–278, https://doi.org/10.1016/0197-4580(95)00021-6.

[74] M.B. Hansen, S.E. Nielsen, K. Berg, Re-examination and further development of a precise and rapid dye method for measuring cell growth/cell kill, J. Immunol. Methods 119 (1989) 203–210, https://doi.org/10.1016/0022-1759(89)90397-9.

[75] O. Quehenberger, T. Yamashita, A.M. Armando, E.A. Dennis, W. Palinski, Effect of gestational hypercholesterolemia and maternal immunization on offspring plasma eicosanoids, Am. J. Obstet. Gynecol. 205 (2011) 156, https://doi.org/10.1016/j.ajog.2011.03.044, e15-25.

[76] M.Y. Pai, B. Lomenick, H. Hwang, R. Schiestl, W. McBride, J.A. Loo, et al., Drug affinity responsive target stability (DARTS) for small-molecule target identification, Methods Mol. Biol. 1263 (2015) 287–298, https://doi.org/10.1007/978-1-4939-2269-7_22.

[77] L. Carlisle-Moore, C.R. Gordon, C.A. Machutta, W.T. Miller, P.J. Tonge, Substrate recognition by the human fatty-acid synthase, J. Biol. Chem. 280 (2005) 42612–42618, https://doi.org/10.1074/jbc.M507082200.